Optimal Altitude Selection of Aerial Base Stations to Maximize Coverage and Energy Harvesting Probabilities: A Stochastic Geometry Analysis

Saeede Enayati, Hamid Saeedi, Hossein Pishro-Nik, and Halim Yanikomeroglu

***Abstract*—This paper provides radio frequency (RF) energy harvesting and coverage probability analysis using stochastic geometry in a two-hop communication network. In the first hop, terrestrial base stations (TBSs) transmit RF energy and data to the aerial base stations (ABSs) and in the second hop, ABSs forward the data to the user. Numerical results show that the energy harvesting and coverage probabilities can be maximized at almost the same altitude of the ABSs with respect to the TBSs height for low TBSs densities. However, as the density of the backhaul nodes and the energy harvesting sub-timeslot increases, energy harvesting probability improves while coverage probability monotonically decreases by increasing the ABSs height.**

***Index Terms*—Aerial base stations (ABS), energy harvesting, stochastic geometry, coverage probability.**

I. Introduction

Providing a ubiquitous coverage is of vital importance in communication systems. In this regard, aerial base stations (ABSs) have been considered as a temporarily deployable communication network for data supplying and collecting in urban, rural and hard-to-reach areas in both uplink and downlink scenarios. Stochastic geometry, as a powerful analysis tool, has been recently applied to the ABS networks to provide system level analysis [1]–[3] following its successful application to analyze terrestrial base stations (TBSs).

Coverage probability was obtained in [1] assuming a finite network of ABSs modeled as binomial point process (BPP). In [2], secrecy rate analysis of Matérn hardcore point process (MHCP) has been investigated. Assuming a heterogeneous network of terrestrial base stations and ABSs, coverage and rate analysis was analyzed in [3]. The authors of current paper proposed a stochastic trajectory processes for which instantaneous uniform placement of moving ABSs will be maintained in a finite circular area leading to an almost uniform coverage throughout the cell [4].

An important issue to consider in ABS networks is the backhaul link specifications and how it influences the system level performance. Due to the impossibility of using wired links as backhaul for ABSs, wireless solutions such as free space optics (FSO) or mmWave links have been considered. However, these solutions cannot provide reliable backhaul links for the ABS networks when ABSs are moving or when there is an outage due to weather conditions for the case of FSO. Hence, wireless RF links seem to be a better choice for ABS network backhauling [5]. In many cases, TBSs already in place, are deployed to act also as backhaul RF links. In such scenarios, it is expected that the resulting coverage is highly dependent on the height of ABSs for a given density of the TBS network. In this paper, we provide a stochastic geometry based analysis to investigate this hypothesis. We show that for a given density and height of the TBS network, there is an optimal value for the height of the ABSs.

Another important issue in ABS networks is their short life time of 25–30 minutes due to energy limitations [6]. Hence, any improvement in energy consumption can have a favorable effect on increasing the network lifetime [6]. In this regard, it would be beneficial to let the communication systems power requirements of the ABSs be provided by external sources. However, so far, few works paid attention to this issue. The authors in [7] consider solar energy arrival modeled as an independent identically distributed Bernoulli process in a single-hop ABS network. Solar powered UAVs were also considered in [8] to investigate the optimal 3D trajectory and wireless resource allocation in a multi-carrier single-hop ABS network. In line with solar and wind, RF energy harvesting has been suggested to be an alternative power source to batteries, in which DC power can be extracted from the received electromagnetic waves using RF-to-DC power conversion modules. Hence, in this paper, we propose to deploy ambient RF energy harvesting by the ABSs similar to the case of IoT networks [9].

As far as RF energy harvesting in ABSs are concerned, outage probability of a single source-relay-destination network was obtained in [10]. Also, the authors of [11] considered a single source and destination network with multiple energy harvesting UAVs as relays where the channel between the nodes are modeled by fading only.

In this paper, unlike previous works that considered either a single-hop communication with ABSs, or a two-hop communication with single source, relay, and destination, we aim to evaluate the performance of an ABS network where it is backhauled with a TBS network. To the best of our knowledge, this is the first work to consider both the energy harvesting and the coverage probability analysis in a two-hop multiple ABS communication network. Hence, network parameters such as ABSs height with respect to the TBSs' and harvesting time duration are obtained so as to maximize the probability of harvesting, defined as the fraction of timeslots for which we can harvest enough energy that is sufficient for the transmission on the same timeslot.

In our system model, we consider a two-hop communication system: The first hop consists of the two sub-timeslots devoted to energy harvesting and data transmissions from TBSs to the ABSs, respectively; the second hop is associated to the third sub-timeslot to forward the data from ABSs to the end user. It is important to note that the existence of LOS increases the energy harvesting probability in a given timeslot. Increasing the LOS probability can be achieved by increasing the height of the ABSs. On the other hand, such an increase may have an inverse effect on the amount of harvested energy due to the path-loss. In other words, there is a trade-off between maximizing the LOS probability and minimizing the path-loss. In this paper, using stochastic geometry, we investigate and analyze such trade-off. Our analysis show that there is in fact an optimal height of the ABSs that maximizes the energy harvesting probability.

Given the above discussion, an important question arises: should a compromise be made in the height of the ABSs in case we want

Manuscript received March 6, 2019; revised September 2, 2019; accepted September 30, 2019. Date of publication October 31, 2019; date of current version January 15, 2020. This work was supported by NSF Grant CNS 1932326. The review of this article was coordinated by Dr. S. Misra. *(Corresponding author: Hamid Saeedi.)*

S. Enayati and H. Pishro-Nik are with the Electrical and Computer Engineering Department, University of Massachusetts, Amherst, MA 01003 USA (e-mail: senayati@umass.edu; pishro@ecs.umass.edu).

H. Saeedi is with the Electrical and Computer Engineering Department, Tarbiat Modares University, Tehran 14115, Iran (e-mail: hsaeedi@ieee.org).

H. Yanikomeroglu is with the Systems and Computer Engineering Department, Carleton University, Ottawa, ON K1S 5B6, Canada (e-mail: halim@sce.carleton.ca).

Digital Object Identifier 10.1109/TVT.2019.2950874

0018-9545 © 2019 IEEE. Personal use is permitted, but republication/redistribution requires IEEE permission.
See http://www.ieee.org/publications_standards/publications/rights/index.html for more information.

Authorized licensed use limited to: University of Massachusetts Amherst. Downloaded on September 05,2020 at 18:44:37 UTC from IEEE Xplore. Restrictions apply.

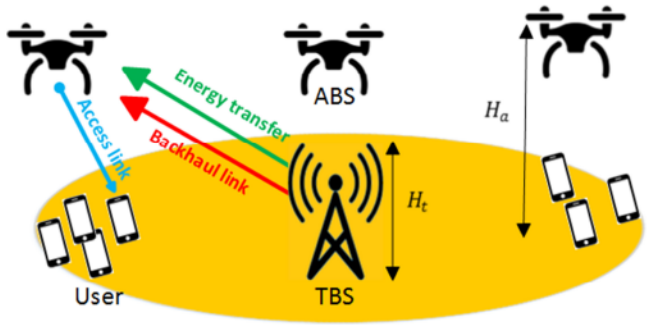

Fig. 1. ABSs as access points for the users and TBSs as backhaul for the ABSs.

to maximize the energy harvesting probability while obtaining the maximum coverage probability. Our analysis shows that for networks with lower density of TBSs, both RF energy harvesting and coverage probabilities are maximized for pretty much the same heights of ABSs. However, we observe that as the density of TBSs increases, RF energy harvesting and coverage probabilities decrease monotonically vs. the ABSs height. We show that with proper adjustment of ABS heights, we can practically provide almost all required transmit power through energy harvesting which can, in turn, increase the flying time of the ABSs.

This paper is organized as follows: Section II introduces system model and initial parameters as well as some primary formulations. Section III provides the coverage probability analysis and Section IV presents the numerical results.

II. System Model Descriptions

We consider a timeslot-based network in which ABSs first harvest ambient RF energy from the TBSs and then use it to receive and transmit data, respectively. Specifically, each timeslot of length T is partitioned in to three sub-timeslots of lengths $T_h = \rho_1\, T, T_r = \rho_2\, T$, and $T_t = \rho_3\, T$ for harvesting ambient RF energy, receiving data from the backhaul TBS, and transmitting data to the associated receiver, respectively. Fig. 1 shows a representation of our system model. More details on the spatial and channel characteristics and initial mathematical formulations of the system model are provided in the sequel.

A. Spatial and Channel Model for the Backhaul and Access Networks

We consider a network of TBSs modeled as PPP $\Phi_t \equiv \{x_i\} \subset \mathbb{R}^2, i = 0, 1, 2, \ldots$, with density λ_t where x_i is the 2D location of TBSs. Also, TBSs' height is assumed to be H_t. We also consider a network of ABSs modeled as another PPP $\Phi_a \equiv \{y_i\} \subset \mathbb{R}^2, i = 0, 1, 2, \ldots$ with a density $\lambda_a \gg \lambda_t$ independent of Φ_t hovering at the altitude of H_a over the ground. We also model the user distribution as an independent PPP $\Phi_u \equiv \{z_i\} \subset \mathbb{R}^2, i = 0, 1, 2, \ldots$, with density λ_u where $\lambda_u \gg \lambda_a$, so as to assume that all the TBSs and ABSs are active in their communication timeslot.

For the both backhaul TBS-ABS and access ABS-user links, we assume distance-dependent power law path-loss and Nakagami-m fading. Also, LOS and NLOS probabilities are considered in both backhaul and access links due to the air-to-ground channel model defined for the ABSs. In this regard, for the air-to-ground channel, LOS probability is defined as [12]:

$$P_L(r_{x,y}) = \frac{1}{1 + C\exp(-B(\zeta - C))}, \tag{1}$$

where C and B are the constant values depending on the environment properties. Moreover, in (1), ζ is the elevation angle defined as (in degrees) $\zeta = \frac{180}{\pi}\tan^{-1}(\frac{H'}{r_{x,y}})$, where $H' \in \{\Delta H, H_a\}$ and $\Delta H = H_a - H_t$. Also, the probability of having NLOS link is $P_N(r_{x,y}) = 1 - P_L(r_{x,y})$. Hence, generally path-loss is defined as $l(r_{x_i,y_j}, H') = (r^2_{x_i,y_j} + H'^2)^{\alpha_n/2}$ in which $x_i \in \{\Phi_t, \Phi_a\}, y_j \in \{\Phi_a, \Phi_u\}$, and $n \in \{1, 2\}$ for the backhaul and access links, respectively. Furthermore, LOS and NLOS links consideration results in the following path-loss formulations [12]:

$$l(r_{x_j,y_i}, H') = \begin{cases} \text{LOS} & l_L(r_{x_j,y_i}, H') = (r^2_{x_j,y_i} + H'^2)^{\alpha_n/2} \\ \text{NLOS} & l_N(r_{x_j,y_i}, H') = \mu(r^2_{x_j,y_i} + H'^2)^{\alpha_n/2} \end{cases} \tag{2}$$

where μ is the attenuation factor of the NLOS link. Besides, channel power gains of the link between $\{x_i, y_j\}$ are shown as $h^L_{x_i,y_i}$ and $h^N_{x_i,y_i}$ distributed according to the Gamma$(m, \frac{1}{m})$ PDF with $m \in \{m_L, m_N\}$ for the LOS and NLOS links, respectively, assumed to be integers for the sake of tractability.

B. Harvested Energy and SIR Definition

Using the assumptions above, in this section we define energy harvested by a typical ABS and the signal-to-interference ratios (SIRs). Since the total amount of energy harvested by the ABS from TBSs is a power-law shot noise process with unknown probability distribution function (PDF) [9], we only consider the energy harvested by the ABS from its nearest TBS as the dominant RF transmitter and take into account the other TBSs' energy harvested as a constant value. This assumption was previously applied in RF-powered IoT-based networks in [13]. Hence, assuming the nearest ABS to the user is located at y_0 and the nearest TBS to the corresponding ABS is located at x_0, the harvested amount of RF energy in the first sub-timeslot, i.e., $T_h = \rho_1\, T$, can be defined as

$$E(r_{x_0,y_0}) \approx \eta T_h P_{t_h} \times \left(\sum_{q\in Q} \frac{P_q(r_{x_0,y_0})h^q_{x_0,y_0}}{l_q(r_{x_0,y_0}, \Delta H)} + \bar{E}(r_{x_0,y_0}, r_{y_0,0})\right), \tag{3}$$

where P_{t_h} is the transmit power from the TBSs for the RF ambient energy harvesting (assumed to be the same for all the TBSs), η ($0 < \eta < 1$) is the RF harvested energy to DC conversion efficiency, and $Q = \{L, N\}$. Furthermore, $\bar{E}$ is the average received RF power from the other TBSs which are farther than the nearest one located at x_0.

We assume ABSs consume all the amount of energy harvested in the first sub-timeslot during the next other two if it is greater than a certain energy threshold, $E_{\min} = E_0 + T_t P_{t_2}$ where E_0 is the required energy for the data receiving and decoding defined as $E_0 = T_r(a\log_2(1 + \gamma_b) + b)$ similar to [9] in which γ_b is the minimum required SIR at the ABS and a and b are constants. Furthermore, $T_t P_{t_2}$ is the required power to transmit data to the typical user. Therefore, the probability that an ABS harvests enough energy for the subsequent sub-timeslot, referred to as energy harvesting probability, is obtained as $P_h = \mathbb{P}(E \geq E_{\min})$.

The received (SIR) from the nearest ABS, to which we refer as the tagged ABS, to the typical user located at the origin in the access link is

$$\text{SIR}_a = \frac{h_{y_0,0}\, l(r_{y_0,0}, H_a)^{-1}}{\sum_{y_i\in\Phi'_a\setminus y_0} h_{y_i,0}\, l(r_{y_i,0}, H_a)^{-1}}, \tag{4}$$

where Φ'_a is the point process with $\lambda'_a = P_h\lambda_a$ produced from Φ_a, assuming the ABSs have harvested enough energy. Hence, conditional

Authorized licensed use limited to: University of Massachusetts Amherst. Downloaded on September 05,2020 at 18:44:37 UTC from IEEE Xplore. Restrictions apply.

access coverage probability is defined as

$$P_a = \mathbb{E}_{r_{y_0,0}} \mathbb{P}(\text{SIR}_\text{a} \geq \gamma_a \mid r_{y_0,0}), \tag{5}$$

where γ_a is the SIR threshold at the access link. Similarly, at the backhaul side, assuming the nearest TBS (tagged TBS) is located at x_0, the received SIR to the tagged ABS located at y_0 is

$$\text{SIR}_\text{b} = \frac{h_{x_0,y_0} l(r_{x_0,y_0}, \Delta H)^{-1}}{\sum_{x_i \in \Phi_t \setminus x_0} h_{x_i,y_0} l(r_{x_i,y_0}, \Delta H)^{-1}}, \tag{6}$$

and the backhaul coverage probability is $P_b = \mathbb{E}_{r_{x_0,y_0}} \mathbb{P}(\text{SIR}_\text{b} \geq \gamma_b \mid r_{x_0,y_0})$.

III. Coverage Probability Analysis

In this section, we analyze the network performance in terms of the coverage probability of the typical user. The coverage probability is formulated as follows:

$$\mathcal{P}_\text{cov} = \mathbb{E}_{r_{x_0,y_0}, r_{y_0,0}} \left[\mathbb{P}(E \geq E_\text{min} \mid r_{x_0,y_0}) \right.$$
$$\left. \mathbb{P}\left(\text{SIR}_\text{b} \geq \gamma_b \mid r_{x_0,y_0}\right) \mathbb{P}\left(\text{SIR}_\text{a} \geq \gamma_a \mid r_{y_0,0}\right) \right], \tag{7}$$

where we note that RF energy harvesting probability and the backhaul coverage probability are conditionally independent [9]. To calculate (7), in the following subsections, we first find the conditional probabilities.

A. Energy Harvesting Probability

Considering Eq. (3), we provide energy harvesting probability in the following lemma:

Lemma 1: Energy harvesting probability as a function of r_{x_0,y_0} is obtained as:

$$P_h(r_{x_0,y_0}) = \sum_{q \in Q} P_q(r_{x_0,y_0}) e^{-m_q z_q} \sum_{k=0}^{m_q - 1} \frac{(m_q z_q)^k}{k!}, \tag{8}$$

where z_q is given by (13).

Proof: See Appendix A. ■

Corollary 1: Integrating of (8) over r_{x_0,y_0} gives us the probability of energy harvested by a typical ABS.

In the following sections, we will go through the backhaul and access coverage probabilities, respectively.

B. Backhaul Coverage Probability

Lemma 2: Backhaul coverage probability of the tagged ABS as a function of r_{x_0,y_0} is obtained as (9), shown at the bottom of this page, where $\mathcal{L}_{I_b}(s)$ is the Laplace transform of the TBSs interference.

Proof: Considering $P_L(r_{x_0,y_0})$ and $P_N(r_{x_0,y_0})$, and the fact that LOS and NLOS propagations have different path-losses and channel power gains, the coverage probability is obtained similar to [14, Theorem 1]. Furthermore, $\mathcal{L}_{I_b}(s)$, shown in (10) at the bottom of this page, is obtained similar to Theorem 1 of [14]. ■

C. Access Coverage Probability

Following (5), we further obtain the coverage probability of the access link in the next lemma:

Lemma 3: Access coverage probability as a function of $r_{y_0,0}$ is obtained similar to (9) where $\mathcal{L}_{I_b}(s)$ is substituted with the Laplace transform of I_a obtained similar to (10), shown at the bottom of the page.

Proof: The proof is similar to the backhaul coverage probability. Note that $\mathcal{L}_{I_a}(s)$ is the Laplace transform of the interference from the ABSs that harvested enough RF energy. ■

Before providing the overall coverage probability analysis, we first need to obtain the PDF of the random variable r_{x_0,y_0} in the following lemma:

Lemma 4: Let $R = r_{x_i,y_0}$. The PDF of the random variable $r_{x_0,y_0} = \min_{x_i \in \Phi_t} r_{x_i,y_0}$ can be obtained as below:

$$f_{r_{x_0,y_0}}(r) = 2\pi\lambda_t r e^{-\pi\lambda_t r^2}. \tag{11}$$

Proof: See Appendix B. ■

Now with the probability terms of Equation (7) calculated in Lemmas 1-3, we obtain the coverage probability through the following theorem:

Theorem 1: The coverage probability of a harvesting ABS-aided network is given by

$$\mathcal{P}_\text{cov} = \mathcal{P}_1(\gamma_b)\mathcal{P}_2(\gamma_a), \tag{12}$$

where $\mathcal{P}_1(\gamma_b) = \int_0^\infty P_h(r_{x_0,y_0}) P_b(r_{x_0,y_0}) f_{r_{x_0,y_0}}(r_{x_0,y_0}) dr_{x_0,y_0}$, $\mathcal{P}_2(\gamma_a) = \int_0^\infty P_a(r_{y_0,0}) f_{r_{y_0,0}}(r_{y_0,0}) dr_{y_0,0}$ and $P_h(r_{x_0,y_0})$, $P_b(r_{x_0,y_0})$, $P_a(r_{y_0,0})$, $f_{r_{x_0,y_0}}(r_{x_0,y_0})$ are provided in Lemmas 1–4, respectively.

Proof: The coverage probability defined in (7) is rewritten as $\mathbb{E}_{r_{x_0,y_0}}[\mathbb{P}(E \geq E_\text{min} \mid r_{x_0,y_0}) \mathbb{P}(\text{SIR}_\text{b} \geq \gamma_b \mid r_{x_0,y_0})] \times \mathbb{E}_{r_{y_0,0}}[\mathbb{P}(\text{SIR}_\text{a} \geq \gamma_a \mid r_{y_0,0})]$, since the random variables r_{x_0,y_0} and $r_{y_0,0}$ can be assumed almost independent [15]. So, deconditioning over r_{x_0,y_0} and $r_{y_0,0}$ results in (12). ■

IV. Numerical Results

In this section, RF energy harvesting and coverage probability are investigated in the presence of LOS and NLOS two hop ABS network. In the simulations, $P_{th} = 1, P_{t_2} = 0.5, \alpha_1 = \alpha_2 = 4, m_L = 3, m_N = 2$, $\mu = 20$ dB, $B = 0.136$, $C = 11.95$, $T = 1$ ms, $\eta = 0.1$, $\lambda_t = 1$, $\gamma_b = -10$ dB, $\gamma_a = -20$ dB, $\rho_2 = 0.6 - \rho_1, \rho_3 = 0.4$, and $\lambda_a = 10\lambda_t$. Also, in the figures, diamonds and triangles show the simulation results

$$P_b(r_{x_0,y_0}) = P_L(r_{x_0,y_0}) \sum_{k=0}^{m_L - 1} \frac{(-s)^k}{k!} \frac{d^k}{ds^k} \mathcal{L}_{I_b}(s) \mid_{s = m_L \gamma_b l_L(r_{x_0,y_0}, \Delta H)} + (1 - P_L(r_{x_0,y_0}))$$
$$\times \sum_{k=0}^{m_N - 1} \frac{(-s)^k}{k!} \frac{d^k}{ds^k} \mathcal{L}_{I_b}(s) \mid_{s = m_N \gamma_b l_N(r_{x_0,y_0}, \Delta H)} \tag{9}$$

$$\mathcal{L}_{I_b}(s) = \exp\left(-2\pi\lambda_c \int_{r_{x_0,y_0}}^\infty \left(1 - \frac{P_L(r)}{\left(1 + \frac{s}{m_L} l_L(r, \Delta H)^{-1}\right)^{m_L}} - \frac{1 - P_L(r)}{\left(1 + \frac{s}{m_N} l_N(r, \Delta H)^{-1}\right)^{m_N}} \right) r dr \right) \tag{10}$$

Authorized licensed use limited to: University of Massachusetts Amherst. Downloaded on September 05,2020 at 18:44:37 UTC from IEEE Xplore. Restrictions apply.

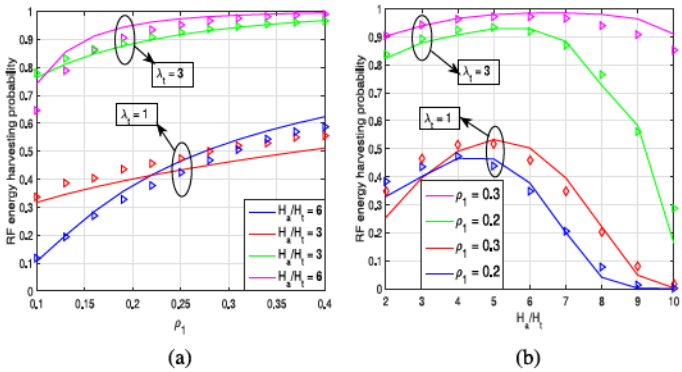

(a) (b)

Fig. 2. Energy harvesting probability. (a) P_h vs ρ_1. (b) P_h vs H_a/H_t.

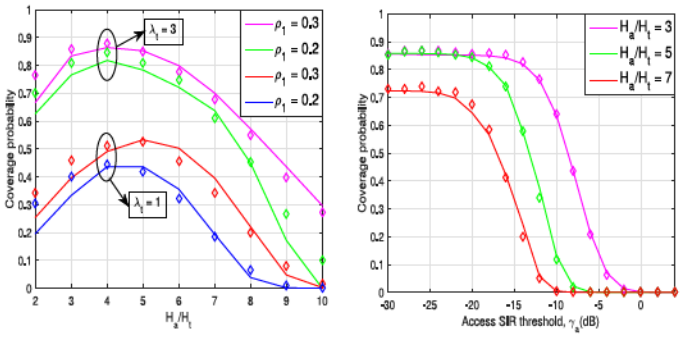

(a) (b)

Fig. 3. Coverage probability. (a) $\mathcal{P}_{cov}$ vs H_a/H_t for $\lambda_t = 1, 3$ and $\rho_1 = 0.2, 0.3$. (b) $\mathcal{P}_{cov}$ vs γ_a for different H_a/H_t. $\lambda_t = 3$ and $\rho_1 = 0.3$.

and solid lines show the analysis. More details on the parameters are provided in the figure captions.

Fig. 2a shows RF energy harvesting probability versus the harvesting fraction of the time-slot, ρ_1, for two values of ABSs heights and TBSs densities.

As might have been expected, increasing energy harvesting sub-timeslot improves RF energy harvesting probability. It also shows λ_t has a positive effect on the energy harvesting probability. Besides, increasing the ABSs height, H_a, reduces the RF energy harvesting probability. However, this reduction becomes less as ρ_1 increases. Nevertheless, as ρ_1 cannot be that much, the height differences matters. Furthermore, assumption of LOS probability results in the existence of an optimal value for H_a which results in a maximum energy harvesting probability in the low values of λ_t and ρ_1. This has been represented in Fig. 2b. According to this figure, it can be observed that increasing λ_t results in a higher energy harvesting probability. Furthermore, the effect of ABSs altitude becomes faint when both λ_t and ρ_1 are large, i.e., $\lambda_t = 3$ and $\rho_1 = 0.3$. It also can be perceived from this figure that for relatively high density of TBSs, selecting the smaller values of ρ_1 will be sufficient to achieve a desirable energy harvesting probability level.

As the coverage probability is the main performance metric to be concerned about, in Fig. 3a we show the coverage probability vs. H_a. In this figure, similar to the energy harvesting probability, in the low values of λ_t and ρ_1, the coverage probability is maximized with respect to $\frac{H_a}{H_t}$ where for example in blue and red curves of this figure the maximum values happen at $\frac{H_a}{H_t} = 4$ and $\frac{H_a}{H_t} = 5$, respectively.

Furthermore, coverage probability has been demonstrated in Fig. 3b where it shows a decreasing attitude when the access SIR threshold, γ_a, increases. Furthermore, the effect of H_a is also demonstrated in this figure, where it shows decreasing H_a results in the improvement in coverage probability performance since for the higher values of λ_t and ρ_1, which are 3 and 0.3 in this figure, coverage probability monotonically decreases as H_a increases.

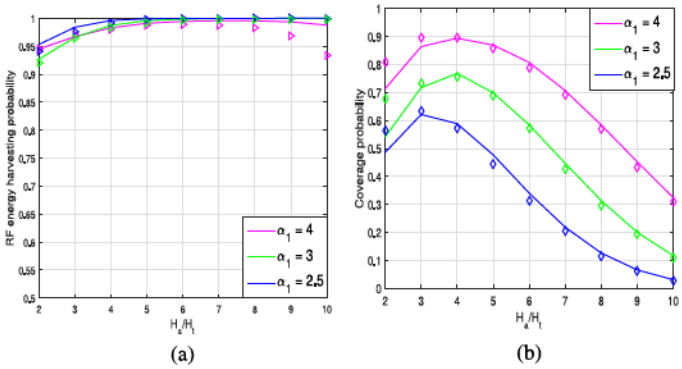

(a) (b)

Fig. 4. Energy harvesting and coverage probability for different values of backhaul path-loss exponent. (a) P_h vs H_a/H_t for $\alpha_1 = 2.5, 3, 4$. (b) $\mathcal{P}_{cov}$ vs H_a/H_t for $\alpha_1 = 2.5, 3, 4$.

Finally, Fig. 4 represents energy harvesting and coverage probabilities for different values of the path-loss exponent in the backhaul link, i.e., the link from the TBSs to the ABSs. In these figures, $\alpha_2 = 4$, $P_{t_h} = 1$, $P_{t_2} = 0.5$ and $\rho_1 = 0.3$. Also, we assume that $\rho_2 = 0.7 - \rho_1$ so that equal sub-timeslots are allotted to the power harvesting and transmitting by the ABSs. Fig. 4a shows that energy harvesting probability increases monotonically as the $\frac{H_a}{H_t}$ increases. Also, it shows that a decrease in the path-loss exponent of the backhaul link will increase the energy harvested by the ABS. However, in Fig. 4b, it can be observed that coverage probability decreases as the path-loss exponent decreases. This is due to the fact that we assumed an interference-dominant network with the minimum distance association policy where SIR decreases with the decrease of path-loss exponent. Hence, despite improving the energy harvesting probability, path-loss exponent decrease has an adverse effect on the coverage probability. This, certainly, is not the case in a network without interference.

V. Conclusion

In this paper, we investigated the RF energy harvesting and coverage probability of a two hop ABS-aided communication system where optimal values of ABSs height for the best RF energy harvesting and coverage probability performance were obtained. It was observed that increasing the harvesting time duration improves energy harvesting and coverage probabilities. These two performance metrics improve for larger TBSs densities. For fixed values of densities, optimal heights to maximize energy harvesting and coverage probabilities were obtained. It was shown that for networks with lower density of TBSs, both RF energy harvesting and coverage probabilities are maximized for approximately the same heights of ABSs. It was also shown that with proper adjustment of ABS height, we can practically provide almost all required transmit power through energy harvesting. As an extension of this work, the performance of energy harvesting can be improved even more by deploying multiple-antennas in a beam-forming scheme.

Appendix A
Proof of Lemma 1

Conditioned on the LOS and NLOS propagations, energy harvesting probability is $P_h(r_{x_0,y_0}, q) = \mathbb{P}(h^q_{x_0,y_0} \geq z_q \mid q) \overset{(a)}{=} 1 -$

Authorized licensed use limited to: University of Massachusetts Amherst. Downloaded on September 05,2020 at 18:44:37 UTC from IEEE Xplore. Restrictions apply.

$\frac{\Gamma(m_q, m_q z_q)}{\Gamma(m_q)} = e^{-m_q z} \sum_{k=0}^{m_q-1} \frac{m_q z^k}{k!}$, where (a) holds since h_{x_0,y_0} is a Gamma random variable and

$$z_q = \left[l_q(r_{x_0,y_0}, \Delta H) \left(\frac{E_0}{\eta T_h P_{th}} + \frac{\rho_3 P_{t_2}}{\eta \rho_1 P_{th}} - \bar{E}(r_{x_0,y_0}) \right) \right]^+, \tag{13}$$

where $[.]^+ = \max(0, .)$ and $\bar{E}(r_{x_0,y_0})$ is obtained as

$$\mathbb{E}\left[\sum_{x_i \in \Phi_t \setminus x_0} \sum_{q \in Q} P_q(r_{x_i,y_0}) l_q(r_{x_i,y_0}, \Delta H)^{-1} | x_0, y_0 \right] \overset{(b)}{=}$$
$$2\pi\lambda_t \left(\int_{r_{x_0,y_0}}^{\infty} \left(\frac{P_L(r)}{(r^2 + \Delta H^2)^{\alpha_1/2}} + \frac{P_N(r)}{\mu(r^2 + \Delta H^2)^{\alpha_1/2}} \right) r dr \right), \tag{14}$$

where the first line comes from averaging over the channel power gain which is $\frac{m_q}{m_q} = 1$ and (b) results from the well-known Campbell theorem.

Appendix B
Proof of Lemma 4

Using the displacement theorem of PPPs [16], the intensity measure of the point process $R = r_{x_i,y_0}$ is $\Lambda_R([0,t)) = 2\pi\lambda_t \int_0^t r dr = \pi\lambda_t t^2$.

Hence, applying the null probability of the random variable $r_{x_0,y_0} = \min R$, we obtain $F_{r_{x_0,y_0}} = \Pr(r_{x_0,y_0} < t) = 1 - e^{-\Lambda_R([0,t))} = 1 - e^{-\pi\lambda_t t^2}$, derivation of which results in (11).

References

[1] V. V. Chetlur and H. S. Dhillon, "Downlink coverage analysis for a finite 3D wireless network of unmanned aerial vehicles," *IEEE Trans. Commun.*, vol. 65, no. 10, pp. 4543–4558, Oct. 2017.

[2] Y. Zhu, G. Zheng, and M. Fitch, "Secrecy rate analysis of UAV-enabled mmwave networks using Matérn hardcore point processes," *IEEE J. Sel. Areas Commun.*, vol. 36, no. 7, pp. 1397–1409, Jul. 2018.

[3] M. Alzenad and H. Yanikomeroglu, "Coverage and rate analysis for vertical heterogeneous networks (VHetNets)," Nov. 2018. [Online]. Available: https://www.researchgate.net/publication/329197079

[4] S. Enayati, H. Saeedi, H. Pishro-Nik, and H. Yanikomeroglu, "Moving aerial base station networks: A stochastic geometry analysis and design perspective," *IEEE Trans. Wireless Commun.*, vol. 18, no. 6, pp. 2977–2988, Jun. 2019.

[5] E. Kalantari, M. Z. Shakir, H. Yanikomeroglu, and A. Yongacoglu, "Backhaul-aware robust 3D drone placement in 5G+ wireless networks," in *Proc. IEEE Int. Conf. Commun. Workshops*, May 2017, pp. 109–114.

[6] L. Gupta, R. Jain, and G. Vaszkun, "Survey of important issues in UAV communication networks," *IEEE Commun. Surv. Tut.*, vol. 18, no. 2, pp. 1123–1152, Apr.–Jun. 2016.

[7] H. Wu, X. Tao, N. Zhang, and X. Shen, "Cooperative UAV cluster-assisted terrestrial cellular networks for ubiquitous coverage," *IEEE J. Sel. Areas Commun.*, vol. 36, no. 9, pp. 2045–2058, Aug. 2018.

[8] Y. Sun, D. Xu, D. W. K. Ng, L. Dai, and R. Schober, "Optimal 3D-trajectory design and resource allocation for solar-powered UAV communication systems," *IEEE Trans. Commun.*, vol. 67, no. 6, pp. 4281–4298, Jun. 2019.

[9] M. A. Kishk and H. S. Dhillon, "Joint uplink and downlink coverage analysis of cellular-based RF-powered IoT network," *IEEE Trans. Green Commun. Netw.*, vol. 2, no. 2, pp. 446–459, Jun. 2018.

[10] L. Yang, J. Chen, M. O. Hasna, and H.-C. Yang, "Outage performance of UAV-assisted relaying systems with RF energy harvesting," *IEEE Commun. Lett.*, vol. 22, no. 12, pp. 2471–2474, Dec. 2018.

[11] B. Ji, Y. Li, B. Zhou, C. Li, K. Song, and H. Wen, "Performance analysis of UAV relay assisted IoT communication network enhanced with energy harvesting," *IEEE Access*, vol. 7, pp. 38 738–38 747, 2019.

[12] A. Al-Hourani, S. Kandeepan, and A. Jamalipour, "Modeling air-to-ground path loss for low altitude platforms in urban environments," in *Proc. IEEE Global Commun. Conf.*, Dec. 2014, pp. 2898–2904.

[13] M. A. Kishk and H. S. Dhillon, "Coexistence of RF-powered IoT and a primary wireless network with secrecy guard zones," *IEEE Trans. Wireless Commun.*, vol. 17, no. 3, pp. 1460–1473, Mar. 2018.

[14] I. Atzeni, J. Arnau, and M. Kountouris, "Downlink cellular network analysis with LOS/NLOS propagation and elevated base stations," *IEEE Trans. Wireless Commun.*, vol. 17, no. 1, pp. 142–156, Jan. 2018.

[15] W. Lu and M. Di Renzo, "Stochastic geometry modeling and system-level analysis & optimization of relay-aided downlink cellular networks," *IEEE Trans. Commun.*, vol. 63, no. 11, pp. 4063–4085, Nov. 2015.

[16] M. Haenggi, *Stochastic Geometry for Wireless Networks*. Cambridge, U.K.: Cambridge Univ. Press, 2012.

Authorized licensed use limited to: University of Massachusetts Amherst. Downloaded on September 05,2020 at 18:44:37 UTC from IEEE Xplore. Restrictions apply.